Video Article

Compact Quantum Dots for Single-molecule Imaging

Andrew M. Smith[1], Shuming Nie[1,2]

[1]Department of Biomedical Engineering, Emory University

[2]Department of Chemistry, Georgia Institute of Technology

Correspondence to: Shuming Nie at snie@emory.edu

URL: https://www.jove.com/video/4236
DOI: doi:10.3791/4236

Keywords: Physics, Issue 68, Biomedical Engineering, Chemistry, Nanotechnology, Nanoparticle, nanocrystal, synthesis, fluorescence, microscopy, imaging, conjugation, dynamics, intracellular, receptor

Date Published: 10/9/2012

Citation: Smith, A.M., Nie, S. Compact Quantum Dots for Single-molecule Imaging. *J. Vis. Exp.* (68), e4236, doi:10.3791/4236 (2012).

Abstract

Single-molecule imaging is an important tool for understanding the mechanisms of biomolecular function and for visualizing the spatial and temporal heterogeneity of molecular behaviors that underlie cellular biology [1-4]. To image an individual molecule of interest, it is typically conjugated to a fluorescent tag (dye, protein, bead, or quantum dot) and observed with epifluorescence or total internal reflection fluorescence (TIRF) microscopy. While dyes and fluorescent proteins have been the mainstay of fluorescence imaging for decades, their fluorescence is unstable under high photon fluxes necessary to observe individual molecules, yielding only a few seconds of observation before complete loss of signal. Latex beads and dye-labeled beads provide improved signal stability but at the expense of drastically larger hydrodynamic size, which can deleteriously alter the diffusion and behavior of the molecule under study.

Quantum dots (QDs) offer a balance between these two problematic regimes. These nanoparticles are composed of semiconductor materials and can be engineered with a hydrodynamically compact size with exceptional resistance to photodegradation [5]. Thus in recent years QDs have been instrumental in enabling long-term observation of complex macromolecular behavior on the single molecule level. However these particles have still been found to exhibit impaired diffusion in crowded molecular environments such as the cellular cytoplasm and the neuronal synaptic cleft, where their sizes are still too large [4,6,7].

Recently we have engineered the cores and surface coatings of QDs for minimized hydrodynamic size, while balancing offsets to colloidal stability, photostability, brightness, and nonspecific binding that have hindered the utility of compact QDs in the past [8,9]. The goal of this article is to demonstrate the synthesis, modification, and characterization of these optimized nanocrystals, composed of an alloyed $Hg_xCd_{1-x}Se$ core coated with an insulating $Cd_yZn_{1-y}S$ shell, further coated with a multidentate polymer ligand modified with short polyethylene glycol (PEG) chains (**Figure 1**). Compared with conventional CdSe nanocrystals, $Hg_xCd_{1-x}Se$ alloys offer greater quantum yields of fluorescence, fluorescence at red and near-infrared wavelengths for enhanced signal-to-noise in cells, and excitation at non-cytotoxic visible wavelengths. Multidentate polymer coatings bind to the nanocrystal surface in a closed and flat conformation to minimize hydrodynamic size, and PEG neutralizes the surface charge to minimize nonspecific binding to cells and biomolecules. The end result is a brightly fluorescent nanocrystal with emission between 550-800 nm and a total hydrodynamic size near 12 nm. This is in the same size range as many soluble globular proteins in cells, and substantially smaller than conventional PEGylated QDs (25-35 nm).

Video Link

The video component of this article can be found at https://www.jove.com/video/4236/

Protocol

The following synthesis procedures involve standard air-free techniques and the use of a vacuum/inert gas manifold; detailed methodology can be found in references 10 and 11. MSDS for all potentially toxic and flammable substances should be consulted before use and all flammable and/or air-labile compounds should be aliquoted into septum-sealed vials in a glove box or glove bag.

1. Synthesis of Mercury Cadmium Selenide ($Hg_xCd_{1-x}Se$) Quantum Dot Cores

1. Prepare a 0.4 M solution of selenium in trioctylphosphine (TOP). Add selenium (0.316 g, 4 mmol) to a 50 ml 3-necked flask, then evacuate and fill with argon using a Schlenk line. Under air-free conditions (dry nitrogen or argon atmosphere), add 10 ml TOP and heat to 100 °C while stirring for 1 hr to yield a clear, colorless solution. Cool the solution to room temperature and set the flask aside.
2. To a 250 ml 3-necked flask, add cadmium oxide (CdO 0.0770 g, 0.6 mmol), tetradecylphosphonic acid (TDPA, 0.3674 g, 1.32 mmol), and octadecene (ODE, 27.6 ml), and evacuate the solution using a Schlenk line while stirring. Increase the temperature to 100 °C and evacuate for an additional 15 min to remove low-boiling point impurities.
3. Under argon or nitrogen gas, heat the mixture to 300 °C for 1 hr to fully dissolve the CdO. The solution will change from a reddish color to clear and colorless. Cool the solution to room temperature.

4. Add hexadecylamine (HDA, 7.0 g) to the cadmium solution, heat to 70 °C, and evacuate. Once a constant pressure is attained, increase the temperature to 100-110 °C and reflux the solution for 30 min. Switch the Schlenk line valve to inert gas and insert the thermocouple directly into the solution.
5. Under air-free conditions, add diphenylphosphine (DPP, 100 µl) to the solution and increase the temperature to 310 °C. Remove 7.5 ml of the 0.4 M TOP-Se solution (3 mmol selenium) in a disposable plastic syringe attached to a 16 gauge needle.
6. Once the temperature equilibrates at 310 °C, set the temperature controller to 0 °C and swiftly inject the TOP-Se solution directly into the cadmium solution. The solution will change from colorless to yellow-orange and the temperature will quickly drop and increase again to ~280 °C. After 1 min of reaction, remove the flask from the heating mantle and quickly cool with a stream of air until the temperature is less than 200 °C.
7. When the temperature reaches ~40 °C, dilute with 30 ml hexane; most of the remaining cadmium precursor will settle out of solution. Remove this precipitate by centrifugation (5,000 x g, 10 min).
8. In each of six 50 ml polypropylene conical centrifuge tube, dilute 12 ml of the crude nanocrystal solution with 40 ml acetone, centrifuge (5,000 x g for 10 min), and carefully decant and discard the supernatant.
9. Dissolve the nanocrystal pellets in hexane (25 ml total volume). Extract this solution 3 times with an equal volume of methanol, retaining the top phase. For the third extraction, the volume of methanol may be adjusted to ~15 ml to obtain a concentrated hexane solution of pure CdSe QDs at roughly 200 µM. The typical yield of this reaction is 3 µmol of CdSe nanocrystals with a diameter of 2.3 nm (50-60% reaction yield).
10. Determine the nanocrystal diameter and concentration by measuring the UV-Vis absorption spectrum and consulting the size-fitting chart of Mulvaney and coworkers [12] and the extinction correlations of Bawendi and coworkers [13]. See Appendix for details.
11. Mercury cation exchange: the nanocrystals may be partially exchanged with mercury to red-shift the absorption and fluorescence emission. Mix the following together in order in a 20 ml glass vial with stirbar (this reaction may be scaled as desired): 3 ml hexane, 2 ml chloroform, 1 ml 200 µM CdSe QD solution (200 nmol), 15 µl oleylamine (OLA), and 500 µl of a 0.1 M solution of $Hg(OT)_2$ in chloroform. Mercury octanethioate ($HgOT_2$) may be prepared by reacting mercury acetate and octanethiol in methanol (see appendix). As the cation exchange reaction proceeds, the extent of red-shift may be monitored with UV-Vis absorption spectrophotometry. After the desired absorption band has been attained, measure the absorption of the nanocrystal solution at 350 nm and determine the new extinction coefficient, assuming that the nanocrystal concentration has not changed (30.7 µM in this example). Quench the reaction by removing the unreacted mercury: add 5 ml decane, 10 ml hexane, and 7 ml methanol and extract the solution, keeping the top phase containing the nanocrystals. Extract twice more with hexane and methanol, and adjust the volume of methanol so that the top phase is ~7 ml. If the phases are slow to separate, the solution may be centrifuged (5,000 x g, 10 min). Add 100 µl TOP, 100 µl OLA, and 100 µl oleic acid to the nanocrystals followed by 40 ml acetone to induce precipitation. Collect the nanocrystals via centrifugation and disperse in 3 ml hexane. Centrifuge again to remove insoluble components and determine the nanocrystal concentration again, using the new extinction coefficient at 350 nm. Allow the nanocrystal solution to age for at least 24 hr at room temperature before proceeding to the next step.

2. Growth of Cadmium Zinc Sulfide ($Cd_yZn_{1-y}S$) Shell

1. Prepare 0.1 M shell precursor solutions in 50 ml 3-necked flasks. Cadmium precursor: cadmium acetate hydrate (230.5 mg, 1 mmol) and 10 ml oleylamine (OLA). Zinc precursor: zinc acetate (183.5 mg, 1 mmol) and 10 ml OLA. Sulfur precursor: sulfur (32.1 mg, 1 mmol) and 10 ml ODE. Under vacuum, heat each solution to reflux for 1 hr to yield clear solutions, and then charge with argon. The sulfur solution may be cooled to room temperature, but the cadmium and zinc precursors are maintained at approximately 50 °C. Calculations of shell precursor quantities can be found in reference 14.
2. Add to a 3-necked flask: $Hg_xCd_{1-x}Se$ QDs (120 nmol, 2.3 nm diameter), ODE (2 ml), and trioctylphosphine oxide (TOPO, 250 mg). Evacuate off the hexane at room temperature using the Schlenk line. Increase the temperature to 100 °C and reflux for 15 min. Change the Schlenk line valve to argon or nitrogen gas and insert the thermocouple in the nanocrystal solution.
3. Increase the temperature to 120 °C, add 0.5 monolayers of sulfur precursor solution (140 µl), and allow the reaction to proceed for 15 min. Small aliquots (<50 µl) may be removed using a glass syringe to monitor the progress of the reaction using fluorescence and/or UV-Vis absorption spectrophotometry. Increase the temperature to 140 °C, add 0.5 monolayers of cadmium precursor solution (140 µl), and allow the reaction to proceed for 15 min. Add 500 µl anhydrous OLA to the reaction solution.
4. At 160 °C add 0.5 monolayers of sulfur precursor solution (220 µl) followed by an equal quantity of zinc precursor solution at 170 °C with 15 min between each addition. Then at 180 °C add 0.25 monolayers of sulfur precursor solution (150 µl) and zinc precursor solution in 15 min intervals.
5. Cool the solution to room temperature and again calculate a new extinction coefficient for these particles using a UV-Vis spectrum, assuming that the number of nanocrystals has not changed (120 nmol in 3.8 ml reaction solution). Store the reaction solution as a crude mixture in a freezer; the nanocrystals may be thawed and purified as needed using the same method described in sections 1.8 and 1.9.
6. The nanocrystals may be characterized using electron microscopy, UV-Vis absorption spectroscopy, and fluorescence spectroscopy. Quantum yield may be calculated absolutely using an integrating sphere or relatively in comparison to a known standard using the methods of reference 15.

3. Phase Transfer

1. Add purified core/shell $Hg_xCd_{1-x}Se/Cd_yZn_{1-y}S$ QDs (5 ml, 20 µM) to a 50 ml 3-necked flask and remove the hexane under a high vacuum to yield a dry film. Fill the flask with argon, add anhydrous pyridine (3 ml) to the nanoparticle film and heat the slurry to 80 °C. Over the course of 1-2 hr the nanoparticles will fully dissolve.
2. Add 1-thioglycerol (1 ml) to the solution and stir at 80 °C for 2 hr. Then cool the solution to room temperature and add triethylamine (0.5 ml) to deprotonate thioglycerol. Stir for 30 min. The solution may become cloudy after the addition of triethylamine due to the poor solubility of polar nanocrystals in this solvent mixture.
3. Transfer the QD solution into a 50 ml conical centrifuge tube containing a mixture of 20 ml hexane and 20 ml acetone, and mix well. Isolate the precipitated nanocrystals via centrifugation (5,000 x g, 10 min), and wash the pellet with acetone.

4. Dissolve the QD pellet in DMSO (5 ml) with bath sonication, and then centrifuge (7,000 x g, 10 min) to remove possible aggregates. Determine the nanoparticle concentration from a UV-Vis absorption spectrum. This solution of pure QDs should be used within 3 hr, as the surface thiols can slowly oxidize under ambient conditions in air.
5. Dilute the QD solution to 10 µM or less with DMSO and transfer to a 50 ml flask. Prepare a 5 mg/ml solution of thiolated polyacrylic acid (synthesis described in Appendix) in DMSO. Add the polymer solution (0.15 mg polymer per nmol QDs) dropwise to the QD solution while stirring and degas the solution at room temperature for 5 min.
6. Purge the QD/polymer solution with argon and heat to 80 °C for 90 min. Then cool the solution to room temperature and dropwise add an equal volume of 50 mM sodium borate, pH 8. Stir for 10 min.
7. Purify the QDs via dialysis (20 kDa cutoff) in 50 mM sodium borate, pH 8, and then concentrate the particles using a centrifugal filter (10 kDa cutoff). Determine the concentration from a UV-Vis absorption spectrum.

4. PEG Coating

1. In a 4 ml glass vial with stirbar, mix 1 nmol QDs in borate buffer with a 40,000 x molar excess of 750 Da monoamino-polyethylene glycol (30 mg, 40 µmol). If a specific chemical functionality is to be added to the nanocrystals (*e.g.* hydrazide or maleimide), it may be introduced by replacing a fraction of the amino-PEG with a heterobifunctional amino-PEG (30% mole fraction typically works well). Dilute the nanocrystal solution to 1 µM with borate buffer. This reaction may be scaled as desired.
2. Prepare a fresh solution of DMTMM (20 mg, 72 µmol) in DMSO (144 µl). This solution can be briefly heated under a stream of warm tap-water or submerged in a bath sonicator to fully dissolve the DMTMM. Quickly add a 25,000 x molar excess of this 0.5 M DMTMM solution (50 µl) to the QD solution and stir at room temperature for 30 min.
3. Repeat step 4.2 four more times to saturate the nanocrystal surface with PEG. Finally, add 200 µl 1 M Tris buffer to quench the reaction and purify the nanocrystals using dialysis, centrifugal filters, or ultracentrifugation.
4. The nanocrystals may be analyzed for monodispersity, hydrodynamic size, and surface charge using liquid chromatography, agarose gel electrophoresis, and fluorescence microscopy. To determine hydrodynamic size and size distribution using an automated liquid chromatography system (GE AKTAprime Plus), use a Superose 6 column, a flow rate of 0.5 ml/min with PBS buffer eluent, and absorption detection at 260 or 280 nm. Compare nanoparticle elution times with those of molecular weight standards. For agarose gel electrophoresis, prepare a 0.5% agarose gel in 50 mM sodium borate buffer (pH 8.5) or 50 mM sodium phosphate buffer (pH 7.4), mix 1 µM samples with 10% glycerol and load into wells, and run at 100 V for 30 min. Image the nanocrystals in the gel using a UV hand wand or UV transilluminator and for fluorescence excitation. To image the nanocrystals at the single molecule level using fluorescence microscopy, dilute the particles to 0.2 nM in 10 mM phosphate buffer, drop 2.5 µl of the solution on a glass coverslip, and carefully place a second coverslip on top of the liquid bead to spread a film between the coverslips. Image the surface-bound particles using a high numerical aperture objective (ideally at least 1.40) in either epifluorescence or TIRF mode with excitation at wavelengths between 400-580 nm and an electron-multiplying CCD camera. Exact imaging parameters will vary between microscopy setup.

Representative Results

Figure 2 depicts representative absorption and fluorescence spectra for CdSe nanocrystals, $Hg_xCd_{1-x}Se$ nanocrystals after cation exchange, and $Hg_xCd_{1-x}Se/Cd_yZn_{1-y}S$ nanocrystals after shell growth. The core CdSe nanocrystals have a quantum yield of fluorescence near 15% (including long-wavelength deep-trap emission) but this efficiency drops to less than 1% after mercury exchange, likely due to charge carrier traps introduced through surface atom disruption [9]. However the growth of a thin shell of $Cd_yZn_{1-y}S$ boosts this efficiency to more than 70%, which is largely maintained after transfer to water (50% is typical). In contrast, $CdSe/Cd_yZn_{1-y}S$ nanocrystals without mercury incorporation lose a substantial fraction of their quantum yield in water unless a thick shell is grown. Thus by incorporating mercury into the core nanocrystal, the small size of the nanocrystal can be maintained (see TEM in **Figure 3**) without sacrificing brightness. It is important to note that capping with $Cd_yZn_{1-y}S$ shifts the spectra to the red due to leakage of the electronic charge carriers into the shell material; this shift is around 20-30 nm for CdSe cores [16], and increases with increasing mercury content in the core (up to 100 nm).

The use of a 2-step phase transfer to water is critical for obtaining a homogeneous population of nanocrystals that do not require further size sorting to remove clusters and aggregates. In the first step, the nanocrystals are transferred to DMSO using 1-thioglycerol, which displaces oleylamine on the surface of the nanocrystal. Thioglycerol is then replaced with a linear multidentate polymer, resulting in highly stable particles with a minimal increase in hydrodynamic size resulting from the organic coating (<4 nm contribution to the hydrodynamic diameter). The size-exclusion chromatogram depicted in **Figure 4a** confirms that the size is similar to that of conalbumin (75 kDa), and after modification with 750 Da amino-PEG, the size is increased to just 12 nm, similar to that of an IgG antibody. PEG modification neutralizes the surface charge, as confirmed in the agarose gel electrophoresis experiment depicted in **Figure 4b**. We routinely use size-exclusion chromatography and gel electrophoresis for quick characterization of size, size distribution, and surface charge. Dynamic light scattering and zeta potentiometry can also be used, however the scattering cross-section of these ultrasmall particles is very small, and we have found that results from commercial instruments are not reproducible. **Figure 5a** shows an epifluorescence micrograph of these nanocrystals deposited on a glass coverslip and excited with 545 nm visible light. These nanocrystals are readily observed at the single-molecule level at 30 frames per second with an electron-multiplying CCD camera. **Figure 5b** shows that the number of fluorescent particles observed in each frame fluctuates over time with continuous excitation; this is due to a combination of blinking and photodegradation. Blinking dominates for the first ~7 min before oxidative photodegradation slowly becomes apparent.

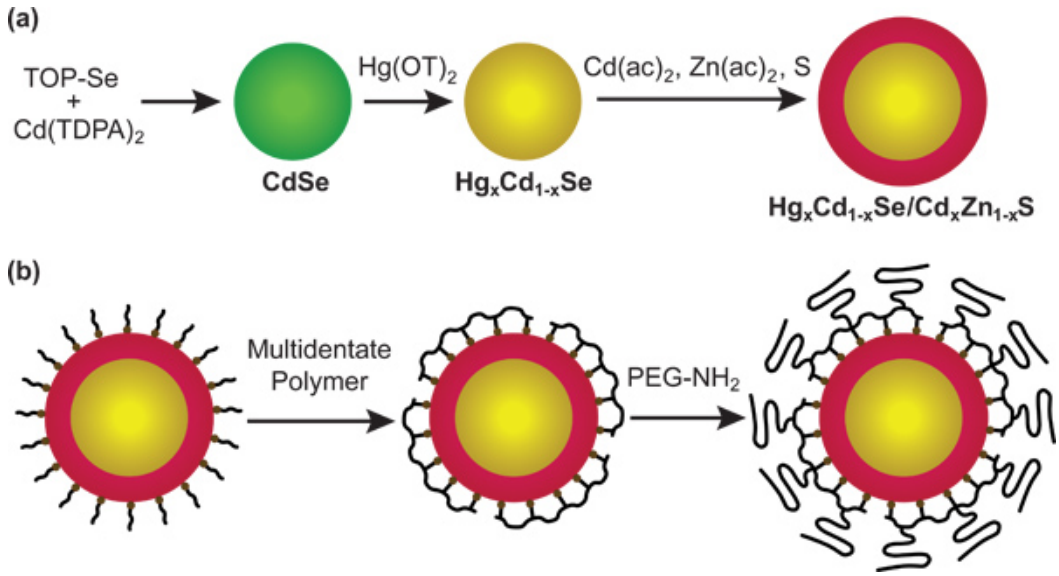

Figure 1. Schematic depiction of the nanoparticle synthesis procedure. (a) Cadmium and selenium precursors react to generate CdSe nanocrystals, which are treated with mercury octanethiolate, inducing partial Cd→Hg cation exchange to yield $Hg_xCd_{1-x}Se$ ternary alloy nanocrystals. A shell of $Cd_yZn_{1-y}S$ is then grown on the core using cadmium acetate, zinc acetate, and sulfur. (b) As synthesized, these nanocrystals are coated with nonpolar organic ligands (oleylamine). To solubilize these particles in aqueous buffers, the ligands are replaced with a multidentate polymer ligand, which is covalently coupled to amino-PEG.

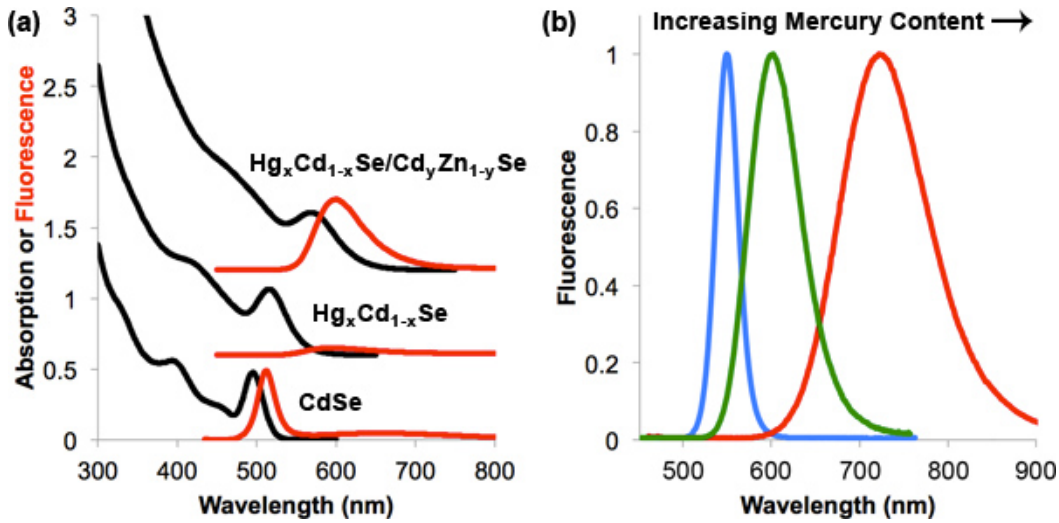

Figure 2. Optical properties of $Hg_xCd_{1-x}Se/Cd_yZn_{1-y}S$ nanocrystals. (a) Absorption (black) and fluorescence spectra (red) of CdSe nanocrystal cores, $Hg_xCd_{1-x}Se$ cores after cation exchange, and $Hg_xCd_{1-x}Se/Cd_yZn_{1-y}S$ nanocrystals after shell growth. Spectra are offset for clarity (b) Fluorescence spectra of $Hg_xCd_{1-x}Se/Cd_yZn_{1-y}S$ with different relative amounts of mercury incorporation. The blue spectrum depicts cores with zero mercury content (x=0, CdSe).

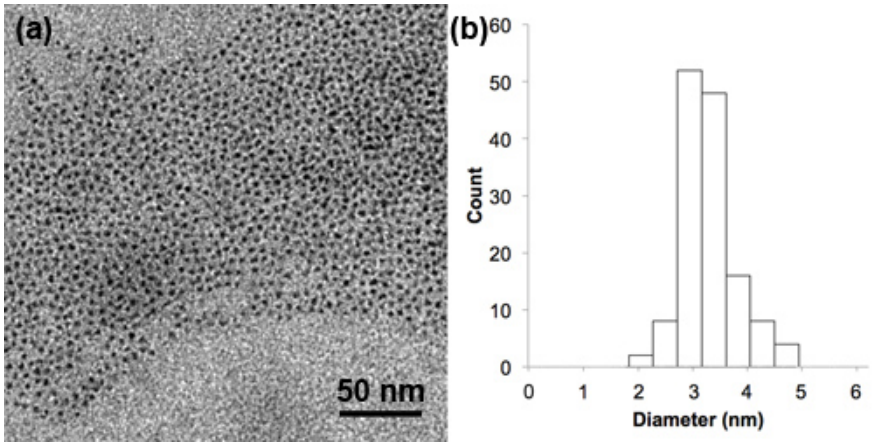

Figure 3. Transmission electron micrograph (a) and particle size distribution (b) of $Hg_xCd_{1-x}Se/Cd_yZn_{1-y}S$ nanocrystals, showing an average diameter ± standard deviation of 3.2 ± 0.6 nm.

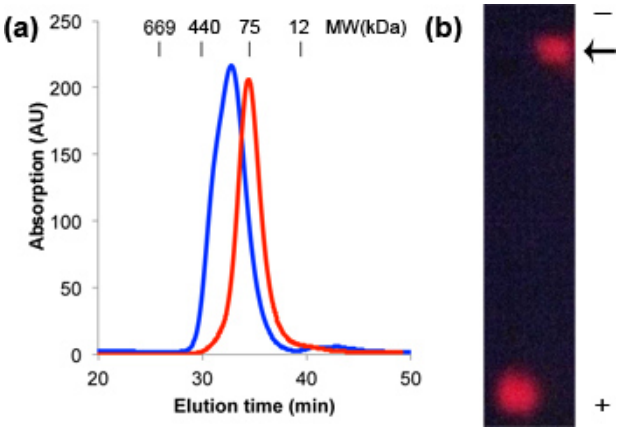

Figure 4. Hydrodynamic characterization of $Hg_xCd_{1-x}Se/Cd_yZn_{1-y}S$ QDs in aqueous solution. (a) Size exclusion chromatogram of nanocrystals coated in a multidentate polymer ligand before (red) and after (blue) conjugation to amino-PEG. Molecular weight protein standards are indicated above the plots. (b) Agarose gel electrophoresis experiment of the QDs in sodium borate buffer (pH ~8.5) before (left) and after (right) conjugation to amino-PEG. The well is marked with an arrow and electrode polarities are indicated on the right, showing that before conjugation the nanocrystals migrate as anionic particles and the PEGylated nanocrystals are electrostatically neutral.

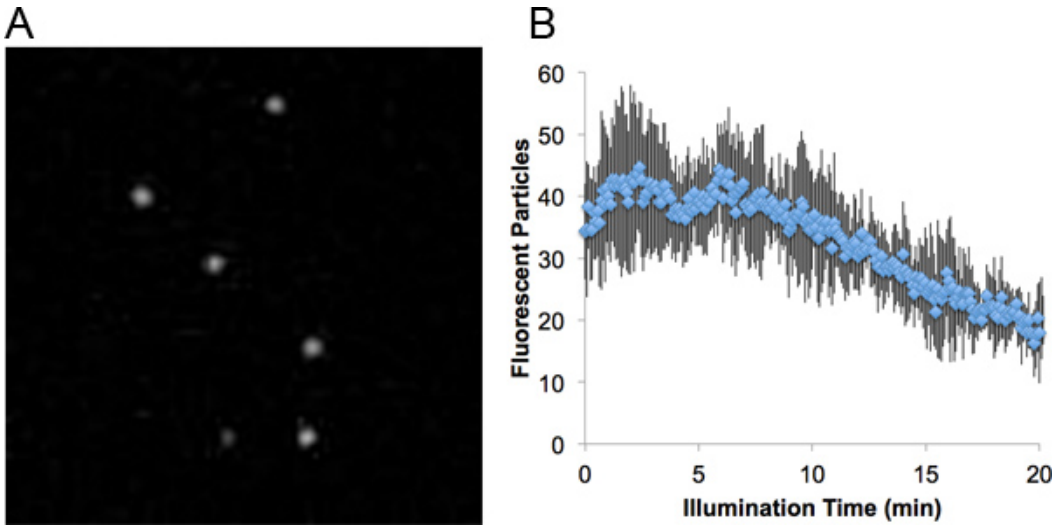

Figure 5. $Hg_xCd_{1-x}Se/Cd_yZn_{1-y}S$ QDs adsorbed on a glass coverslip in phosphate buffer, imaged with epifluorescence microscopy. (a) QD image obtained at 33 frames per second. Image is 15 µm x 15 µm. (b) Number of fluorescent QDs per field of view during continuous illumination for 20 min with mercury arc lamp with 545 nm (30 nm bandpass) excitation filter and a 625 nm (20 nm bandpass) emission filter and 100x 1.4 NA objective. Measurements from 3 fields of view were averaged over 20 min at 12.5 frames per second.

Discussion

Compared to conventional CdSe quantum dots, ternary alloy $Hg_xCd_{1-x}Se$ nanocrystals can be tuned in size and fluorescence wavelength independently. The size is first selected during the synthesis of CdSe nanocrystal cores, and the fluorescence wavelength is chosen in a secondary mercury cation exchange step, which does not substantially alter the nanocrystal size [9]. It is important to allow the purified $Hg_xCd_{1-x}Se$ nanocrystals to incubate at room temperature for at least 24 hours before capping. This allows some of the weakly adsorbed mercury cations to diffuse into the nanocrystal lattice. Without allowing this process to occur, a second fluorescence band in the near-infrared is often observed due to homogeneous nucleation of HgS nanocrystals from dissociated mercury ions.

In the example shown in this work, we prepared CdSe cores with a size near 2.3 nm, which can be tuned in fluorescence between 550-800 nm after capping by altering the amount of mercury incorporated into the core lattice. With a 2.5 monolayer shell, the final diameter of these QDs was near 3.2 nm, which is essentially the smallest size nanoparticle that we can prepare that is both sufficiently photostable and sufficiently bright for single-molecule imaging (extinction coefficient near 350,000 M^{-1} cm^{-1} at 400 nm and quantum yield near 50% in water). These nanocrystals are substantially brighter and more photostable than previously described nanocrystals with comparable sizes that emit over this spectral range (*e.g.* CdTe, InAs, InP). Like most fluorophores, the fluorescence from these particles at the single molecule level is intermittent (blinking) [5,6].

For some applications, it may be beneficial to use somewhat larger nanocrystals. By using a larger CdSe nanocrystal core, the fluorescence bandwidth is narrower after mercury cation exchange. Typical fluorescence peak widths for $Hg_xCd_{1-x}Se$ nanocrystals with emission in the 600-650 nm window are 50-70 nm for 2.3 nm cores and 40-50 nm for 3.2 nm cores. Thereby, larger nanocrystals enable a greater capacity for spectral multiplexing. In addition, increasing the size will likewise increase the absorption cross-section of the nanocrystals. Increasing the thickness of the CdS interim shell layer will also increase the brightness, and further prolong the fluorescence stability during excitation. The CdSe core size may be increased simply by extending the duration of the CdSe core synthesis, and monitoring the effective size through UV-Vis absorption spectrophotometry.

We have found that aqueous QDs coated with carboxylic acids are prone to nonspecific adsorption to cells and proteins, and that neutralization of their strong negative charge in physiological buffers is critical for minimizing nonspecific interactions [17]. In the examples here, we used short-chain PEG to neutralize the surface charge and maintain stability in water. PEG can be introduced into the polymer backbone either before attachment to the QDs or after coating. Both procedures result in nearly neutral particles, but those first coated with the carboxyl-polymer are substantially smaller, presumably due to improved multidentate interaction with the surface. For complete surface neutralization with PEG, we have found that repeated addition of carboxylic acid activating agents is necessary due to the short half-life of the reactive species. We use DMTMM in the place of more common carbodiimide reagents (*e.g.* EDC) because of the improved stability of DMTMM in storage and due to improved reaction efficiency in water [18].

Finally, it is important to note that quantum dots and many other types of nanocrystals contain cytotoxic elements [5]. Cadmium and mercury ions can affect the normal processes of living cells and organisms and may be carcinogenic [19-21]. However the cytotoxicity of conventional CdSe/ZnS nanocrystals has been widely studied and it has been reported that robustly coated nanocrystals with stable organic ligands do not elicit overtly cytotoxic responses compared to their constituent elements, simply because their toxic elements are efficiently sequestered away from oxidizing agents [5]. Moreover, for single-molecule imaging applications, toxic effects are unlikely due to the extremely small concentrations used for imaging (typically 1 nM or less) which are orders of magnitude smaller than the onset of detectable toxic effects (50-100 nM). Most of the single-molecule experiments implementing QDs to date have utilized commercially available CdSe/ZnS nanocrystals, which are substantially larger than those described herein. By minimizing the nanocrystal size, the total number of surface atoms per particle and the total number of toxic atoms per particle are substantially reduced, thereby reducing the total potential for toxicological impact. The incorporation of mercury into the nanocrystal is expected to further reduce the toxicity potential, as divalent mercury is known to be less toxic than divalent cadmium in many cell types [19-21].

Disclosures

No conflicts of interest declared.

Acknowledgements

The authors would like to thank Dr. Hong Yi at the Emory University Integrated Microscopy Core for electron microscopy imaging. This work was sponsored by NIH grants (PN2EY018244, R01 CA108468, U54CA119338, and 1K99CA154006-01).

References

1. Toprak, E. & Selvin, P.R. New fluorescent tools for watching nanometer-scale conformational changes of single molecules. *Annu. Rev. Biophys. Biomol. Struct.* **36**, 349-369 (2007).
2. Joo, C., Balci, H., Ishitsuka, Y., Buranachai, C., & Ha, T.J. Advances in single molecule fluorescence methods for molecular biology. *Annu. Rev. Biochem.* **77**, 51-76 (2008).
3. Pinaud, F., Clarke, S., Sittner, A., & Dahan, M. Probing cellular events, one quantum dot at a time. *Nat. Method.* **7**, 275-285 (2010).
4. Smith, A.M., Wen, M.M., & Nie, S.M. Imaging dynamic cellular events with quantum dots. *Biochemist.* **32**, 12-17 (2010).
5. Smith, A.M., Duan, H.W., Mohs, A.M., & Nie, S.M. Bioconjugated quantum dots for *in vivo* molecular and cellular imaging. *Adv. Drug Deliv. Rev.* **60**, 1226-1240 (2008).
6. Smith, A.M. & Nie, S.M. Next-generation quantum dots. *Nature Biotech.* **27**, 732-733 (2009).

7. Groc, L., Lafourcade, M., Heine, M., Renner, M., Racine, V., Sibarita, J.-B., Lounis, B., Choquet, D., & Cognet, L. Single trafficking of neurotransmitter receptor: comparison between single-molecule/quantum dot strategies. *J. Neurosci.* **27**, 12433-12437 (2007).
8. Smith, A.M. & Nie, S.M. Minimizing the hydrodynamic size of quantum dots with multifunctional multidentate polymer ligands. *J. Am. Chem. Soc.* **130**, 11278-11279 (2008).
9. Smith, A.M. & Nie, S.M. Bright and compact alloyed quantum dots with broadly tunable near-infrared absorption and fluorescence spectra through mercury cation exchange. *J. Am. Chem. Soc.* **133**, 24-26 (2011).
10. Shriver, D.F. & Drezdzon, M.A. *The Manipulation of Air-Sensitive Compounds.*, 2nd edn., Wiley-Interscience, (1986).
11. Errington, R.J. *Advanced Practical Inorganic and Metalorganic Chemistry.*, Blackie, (1997).
12. Jasieniak, J., Smith, L., van Embden, J., Mulvaney, P., & Califano, M. Re-examination of the size-dependent absorption properties of CdSe quantum dots. *J. Phys. Chem. C.* **113**, 19468-19474 (2009).
13. Leatherdale, C.A., Woo, W.K., Mikulec, F.V., & Bawendi, M.G. On the absorption cross section of CdSe nanocrystal quantum dots. *J. Phys. Chem. B.* **106**, 7619-7622 (2002).
14. Smith, A.M., Mohs, A.M. & Nie, S.M. Tuning the optical and electronic properties of colloidal nanocrystals by lattice strain. *Nature Nanotech.* **4**, 56-63 (2009).
15. Demas, J.N. & Crosby, G.A. The measurement of photoluminescence quantum yields. A review. *J. Phys. Chem.* **75**, 991-1024 (1971).
16. Van Embden, J., Jasieniak, J., & Mulvaney, P. Mapping the optical properties of CdSe/CdS heterostructure nanocrystals: the effects of core size and shell thickness. *J. Am. Chem. Soc.* **131**, 14299-14309 (2009).
17. Smith, A.M., Duan, H.W., Rhyner, M.N., Ruan, G., & Nie, S.M. A systematic examination of surface coatings on the optical and chemical properties of semiconductor quantum dots. *Phys. Chem. Chem. Phys.* **8**, 3895-3903 (2006).
18. Zhang, X., Mohandessi, S., Miller, L.W., & Snee, P.T. Efficient functionalization of aqueous CdSe/ZnS nanocrystals using small-molecule chemical activators. *Chem. Comm.* **47**, 3532-3534 (2011).
19. Bucio, L., Souza, V., Albores, A., Sierra, A., Chavez, E., Carabez, A., & Guiterrez-Ruiz, M.C. Cadmium and mercury toxicity in a human fetal hepatic cell line (WRL-68 cells). *Toxicol.* **102**, 285-299 (1995).
20. Han, S.G., Castranova, V., & Vallyathan, V.J. Comparative cytotoxicity of cadmium and mercury in a human bronchial epithelial cell line (BEAS-2B) and its role in oxidative stress and induction of heat shock protein 70. *J. Toxicol. Environ. Health Part A.* **70**, 852-860 (2007).
21. Strubelt, O., Kremer, J., Tilse, A., Keogh, J., & Pentz, R.J. Comparative studies on the toxicity of mercury, cadmium, and copper toward the isolated perfused rat liver. *J. Toxicol. Environ. Health Part A.* **47**, 267-283 (1996).

